

BEHAVIOUR OF CONCRETE IN SEVERE FROST ACTION



M. T. Leivo,
Technical Research Centre of Finland,
Concrete and Silicate Laboratory
Lic.Tech, Research Scientist

ABSTRACT

The freezing and thawing resistance is the most important property of concrete to be used in arctic offshore structures. This paper presents results of a study dealing with freezing and thawing resistance of concrete in arctic offshore conditions. As there was no suitable method for testing of freezing and thawing resistance under arctic conditions, a new method was developed for accelerated testing.

Key-words: Concrete durability, arctic conditions, testing methods, frost resistance.

1. INTRODUCTION

In arctic offshore conditions concrete structures are subjected to severe external factors affecting their durability. The most critical part of a structure is its splash and tidal zone, which lies over the lowest level reached by the waves. This zone is subjected to the following aggressive factors:

- frequently repeated freezing and thawing in a wet state
- chemical attack of sea water
- abrasion of ice, waves and accompanying sand
- thermal stress from tide and waves.

In arctic regions frost attack is more severe than in sub-arctic regions due to the lower temperatures. As the temperature falls, the water freezes in pores of an ever-decreasing size resulting in an increase in internal stress. In the tests /6/ it has been found that during repeated freezing and thawing in the +20...-55 °C temperature range concrete deteriorated much faster than in the +20...-20 °C range. In the Arctic Ocean the lowest air temperatures range from -40...-50 °C.

The freezing and thawing resistance and the strength are the most important properties of concrete for use in arctic offshore structures. This paper presents results of a study

dealing with the freezing and thawing resistance of concrete in arctic conditions. As there was no suitable method for the testing of freezing and thawing resistance under arctic conditions, a new method was developed for accelerated testing.

2. THEORIES ON FROST DAMAGE AND THEIR APPLICATION TO ARCTIC CONDITIONS

Damage to concrete due to repeated cycles of freezing and thawing is a very complicated process that has not yet been fully understood. Several theories have been suggested to explain how concrete is damaged and how such damage could be eliminated.

We will deal with some of the more popular theories on frost resistance and examine how they could be applied to arctic offshore conditions. The theories that we will discuss are the classical hydraulic pressure theory and the capillary ice lens growth theory.

To keep the presentation of these theories relatively simple, the effect of salts has been omitted. No doubt, salts intensify the action of frost on concrete but the mechanism has never been completely cleared up.

2.1 Hydraulic pressure theory

The hydraulic pressure theory is one of the oldest and most common theories used for explaining frost resistance. As T.C. Powers, the first proponent of the theory, has pointed out, it does not always explain damage to concrete /8, 9/. However, it is still one of the most commonly used theories because of its clarity and simplicity.

The hydraulic pressure theory assumes that damage to concrete under frost attack is due to hydraulic pressure caused by the expansion (9 %) of water upon freezing. As the water in a water-filled capillary freezes, some of the unfrozen water must exit through the pore to make room for the ice. Since hardened paste is relatively impermeable, it seeks to prevent the migration of water, which creates a hydraulic pressure that is liable to break the concrete. It should be pointed out that, according to the theory of hydraulic pressure, increasing the impermeability of the concrete will increase the stress acting on it unless the amount of freezing water is not considerably reduced.

Another thing that should be pointed out is that freezing takes place over a very wide temperature range (see Fig. 1). At the same time, the permeability of hardened paste changes during the freezing process. The ice crystals formed in the capillaries tend to block them and so decrease the permeability of the paste.

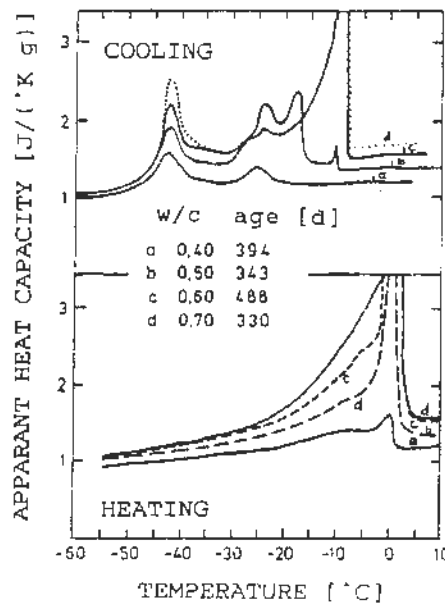


Fig. 1. Ice formation in various hardened concrete pastes as determined by a calorimeter /1/.

By taking into account these factors and using the freezing curve presented in Fig. 1, which represents a water-cement ratio of 0.50, we can calculate the development of hydraulic pressure as shown in Fig. 2. For the calculations, we used a cooling rate of 11°C/h, spacing factor of 0.27 mm and an average radius of air pores of 0.127 mm. The values for water viscosity were obtained from source /4/. Some of the values had to be linearly extrapolated from the values given. For the computation, we used the formula (formula 1) presented in source /11/.

$$P_{\max} = n/K * C * \phi (L), \tag{1}$$

where

$$\phi (L) = L^3/r_b + 3L^2/2 \tag{2}$$

- P_{\max} = maximum value of hydraulic pressure at the given moment
- n water viscosity
- K permeability of the hardened mix
- C ice formation rate
- L spacing factor
- r_b average radius of pores

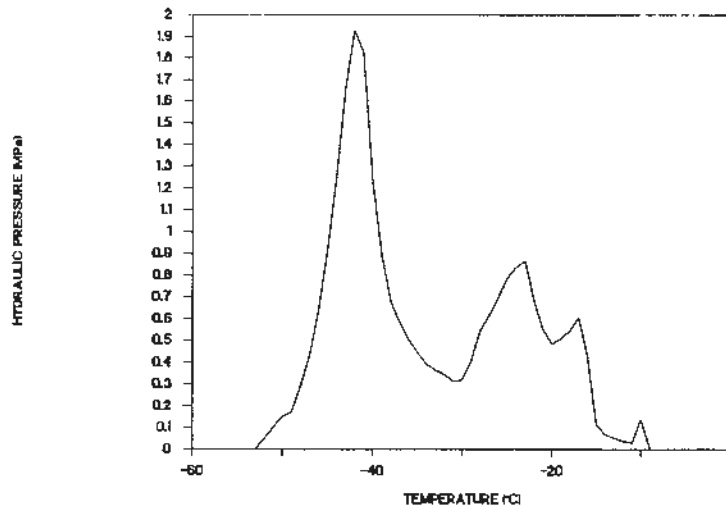


Fig. 2. Increase in hydraulic pressure with decreasing temperature at a water-cement ratio of about 0.50.

The computations would indicate that hydraulic pressure is lower than the strength of concrete. However, it should be pointed out that the strength of the concrete and the stresses caused by the frost attack are, at the micro-level, randomly distributed. So we may easily have a situation even at low average stresses where a high stress and low strength occur at the same point in the concrete, which leads to frost damage.

Effect of the water-cement ratio

For structural reasons, arctic offshore structures are built from concrete with a water-cement ratio of 0.35. When examining the effect of a frost attack on this type of concrete according to the hydraulic pressure theory, we see from Fig. 1 and formula 2 that lowering the water-cement ratio both increases and decreases the intensity of such an attack. A closer analysis reveals that, according to the hydraulic pressure theory, the increased stress caused by the lower permeability of the concrete will result in lower frost resistance if the water-cement ratio is reduced.

The hydraulic pressure theory would indicate that frost resistance is lowered if the water-cement ratio is lowered. As we know, this is not true. We may say that the hydraulic pressure theory contains major errors.

2.2 Capillarc ice lens growth theory

The theory of capillarc ice lens growth postulates, contrary to the hydraulic pressure theory, that water is not expelled from the point of freezing but attracted to it. When an ice crystal is formed in a capillarc pore of the concrete, it

tends to grow by absorbing more water from the surrounding hardened paste. This phenomenon, known as the growth of capillare ice crystals, is the factor that causes the frost attack.

According to the capillare theory, the migration of ice lenses and water takes place on a microscopic scale, whereas macroscopic ice lens formation and water migration take place only in soil types susceptible to frost. Attempts have been made to apply this "frost model" to concrete /3/ but it is commonly believed that hardened concrete is not damaged in the same way. A fresh concrete mix or very new concrete (a couple of hours) may, however, be damaged by frost-heaving /9/.

Fig. 3 shows how Powers explains the migration of moisture as liquid. As the figure shows, the walls of the capillare pores are made up from gel particles. Each gel particle has its own adsorbed water film. It is only this adsorbed water film with a thickness of a few molecules that distinguishes the gel particles from ice. Fig. 3 shows the boundary surface between the ice and the capillary wall.

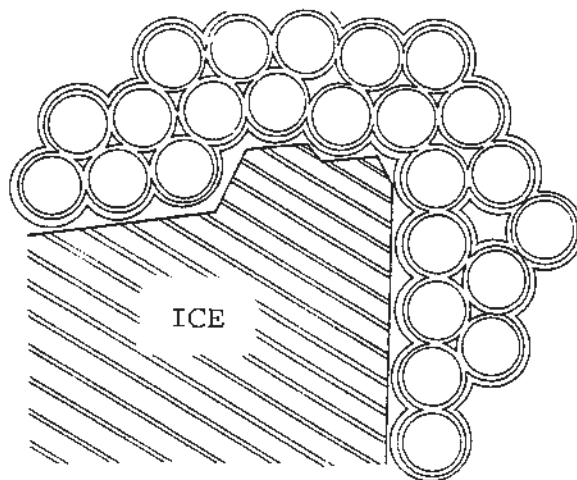


Fig. 3. Wall of a frozen capillare pore /10/.

At certain sub-zero temperatures, the ice crystal is capable of attaching to itself part of the water film and make it thinner than it would otherwise be without the ice crystals. As the temperature continues to drop, more and more molecules move from the film into the ice and the film gets thinner. Because the water film bordering on the capillare pore is identical with the water film adsorbed by the surface of the gel particles (gel water), the thinning of the film causes a difference in chemical energy potential between the water film and the gel water. To reduce this difference in energy, water migrates along the surfaces of the gel particles to the water film of the capillare where there is ice. This process is known as surface diffusion /10/.

The tendency of the hardened paste to shrink as it loses water because of freezing and the growth of the ice lenses produce a

pressure that acts on the ice inside the capillarity pore and its surrounding water film. This pressure increases the chemical energy potential of the ice and the water film and tends to prevent water diffusion from the hardened paste to replace water lost from the water film of the capillary. Pressure keeps increasing until the energy potential of ice is equal to that of the gel water.

According to the theory saying that the moisture migrates in the form of vapour, such migration is explained as being due to the vapour pressure difference between the water and ice /7/. However, it is of little importance whether water migration in the concrete is understood in terms of a vapour pressure difference or differences in chemical energy potential because the vapour pressure difference is anyway due to the difference in chemical energy potential /2/.

An example of the magnitude of the forces involved

If the gel pores remain saturated with water (water is drawn from the surrounding mass or smaller capillaries that have not yet frozen), the pressure change can then be expressed as follows /10/

$$dP = \frac{(S_i - S_w)}{V_i} dT \tag{3}$$

where

- dP = pressure change in the ice crystal
- S_i molar entropy of ice
- S_w molar entropy of water
- V_i molar volume of ice
- dT temperature change.

When putting the values for pure water of about 0 °C into this formula, we obtain

$$\begin{aligned} \frac{dP}{dT} &= \frac{S_i - S_w}{V_i} = \frac{-22 \text{ J/mol}^\circ\text{K}}{19,633 * 10^{-6} \text{ m}^3/\text{mol}} \\ &= -1,12 * 10^6 \text{ J/m}^3 \cdot \text{K} \end{aligned} \tag{4}$$

When ΔT is -1 °K

$$P = 1,12 * 10^6 \text{ N/m}^2.$$

If 6 MPa is used as the tensile strength of the hardened paste (equal to a water-cement ratio of about 0.45), we see that a temperature of only 5.5°C would be sufficient to cause frost damage to the concrete.

This indicates that fairly small temperature drops generate forces sufficiently great to damage even high-strength concrete.

Effect of the air pores

As ice crystals are formed in the concrete, they appear both in the capillarie pores and on the walls of the air pores. Since the ice crystals tend to grow in capillarie pores, they meet with resistance from the concrete, whereas the crystals in the air pores can expand freely. As a result, the chemical energy potential of an ice crystal in an air pore is lower than that of a crystal in a capillarie pore. Because of this difference, the unfrozen water in the concrete tends to migrate to the ice crystal in the air pore rather than to the one in the capillarie pore. This reduces the growth rate of the ice crystal in the capillarie pores and alleviates the severity of the frost attack. If the concrete contains a sufficient number of air pores, the frost attack will be less intense and no damage will occur.

Summary

An equation can be formulated to reflect the effect of the various factors on the frost resistance of concrete. When concrete only just can withstand the frost attack it is subjected to, the following equation is true:

$$f_{pt} = 0,625 * \frac{n(T)}{K} * a^2 * \frac{V_w(T)}{V_i(T)} * \frac{dV_0}{dT} * \frac{dT}{dt} \quad (5)$$

where

- f_{pt} = tensile strength of the concrete
- $n(T)$ water viscosity (depends on temperature)
- a "spacing factor"
- $V_w(T)$ molar water volume
- dV_0/dT migration rate of free water.

When comparing this formula to the formula derived from the hydraulic pressure theory, we see that the formulae are very much the same. No wonder that good results in concrete engineering have been obtained with this theory even though it does not appear completely valid.

As the formula (6) shows, the temperature-dependent variables are viscosity, molar volumes of ice and water and the amount of water drained from the concrete. Fig. 4 shows the dependence of the intensity of the frost attack on temperature at arbitrary values of cooling rate, permeability, A and dV_0/dT .

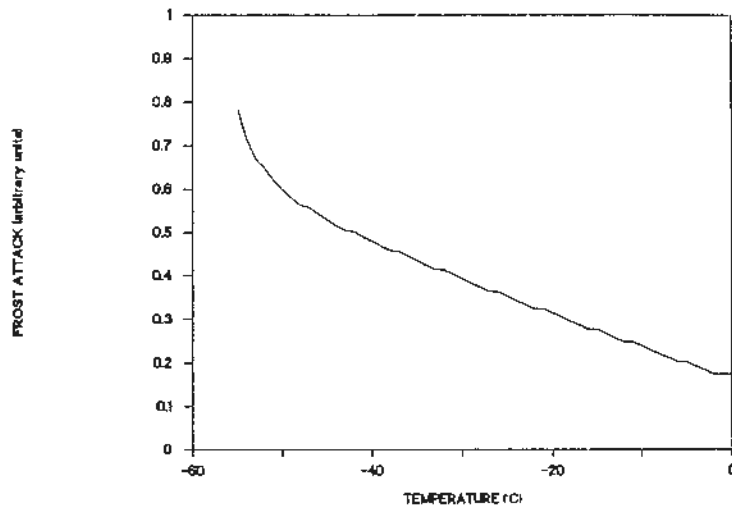


Fig. 4. An example showing the dependance of the intensity of the frost attack on temperature.

3. TEST PROGRAMME

In the test series the freezing and thawing resistance of special concrete mixes for arctic offshore structures was investigated. 31 different superplasticized, high-strength, air-entrained concretes were tested. The following properties of the concretes were studied:

- arctic freezing and thawing resistance
- air content and consistency of fresh concrete
- concrete strength
- pore structure of hardened concrete

The following testing methods were employed:

- automatic optical air pore analysis
- capillary water absorption test
- protective pore ratio test.

4. CONCRETE MIXES

The test specimens were made of 31 concrete mixes. Their compositions are listed in Table 1. Portland cement, slag cement and blended cement were used. About a half of the mixes were made with silica fume. The aggregate used was rounded granite aggregate. The maximum aggregate size was 32 mm.

Table 1. Composition and properties of mixes.

Concrete	Cement : water : aggregate (by weight)	10 min. after mixing		Compressive strength 91 d (150 mm cubes) (MPa)
		Slump (mm)	Air content (%)	
Preliminary mixes:				
Ordinary Portland cement	1 : 0.34 : 3.9	210	3.5	67.0
Portland blast furnace slag cement	1 : 0.35 : 3.9	180	8.3	64.0
Ordinary Portland cement + 8 % silica fume I	1 : 0.35 : 3.9	180	8.0	69.0
- " - II	- " -	210	10.0	55.0
PARTEK I *		150	1.7	66.5
PARTEK II *		160	3.2	66.0
PARTEK III *		140	2.4	79.0
PARTEK IV *		150	7.0	60.0
LIGHTHOUSE **		200	5.0	54.5
Test mixes:				
Portland blast furnace slag cement 1				
- " - 2	1 : 0.35 : 3.98	190	1.8	70.0
- " - 3	- " -	175	3.0	72.5
- " - 4	- " -	205	5.4	64.5
- " - 5	- " -	215	8.8	57.5
- " - 6	- " -	215	10.0	53.0
- " - 7	- " -	265	7.8	51.0
- " - 7	- " -	260	10.3	47.0
Portland blast furnace slag cement + 8 % silica fume 1				
- " - 2	1 : 0.35 : 3.98	145	1.7	82.5
- " - 3	- " -	115	2.7	77.0
- " - 4	- " -	165	4.9	64.5
- " - 5	- " -	200	5.5	68.5
- " - 6	- " -	200	6.2	62.5
- " - 7	- " -	200	7.8	60.5
- " - 7	- " -	170	9.5	53.0
Blended cement *** + 8 % silica fume 1				
- " - 2	1 : 0.35 : 3.98	150	4.0	76.5
- " - 2	- " -	165	8.5	61.5
Ordinary Portland cement 1				
- " - 2	1 : 0.35 : 3.98	140	4.5	58.0
- " - 3	- " -	160	5.7	54.5
- " - 3	- " -	195	7.2	53.5
Ordinary Portland cement + 8 % silica fume 1				
- " - 2	1 : 0.35 : 3.98	185	3.6	70.0
- " - 2	- " -	190	5.4	57.5
- " - 3	- " -	170	7.2	59.5

- *) Test specimens were made by the Partek Corporation.
- **) This concrete was made for the repair of the lighthouse in the Gulf of Finland.
- ***) Blended cement contains 50 % Portland klinker and 50 % blast furnace slag.

5. TESTS

5.1 Freezing and Thawing Test

For testing the freezing and thawing resistance a new method was developed. Specimens (500 * 100 * 100 mm) were submerged in sea water and subjected to repeated freezing and thawing in the temperature range +20...-55 °C. Each specimen was constantly surrounded by a thin layer (~5 mm) of sea water in its own steel container. During the latter part of the thawing phase warm water (+20 °C) was run inside the freezing and thawing box, surrounding the steel containers with warm water. The procedure for one cycle is shown in Figure 5.

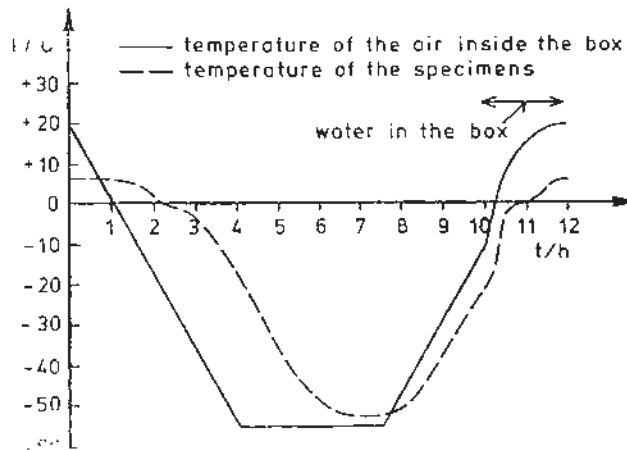


Figure 5. Test procedure during one cycle.

Deterioration was followed by measuring the change in speed of ultrasound through the specimens. The cycles were repeated until the durability factor, which is given by equation 6, was less than 2/3 of the original value. Number of cycles are shown in table 2. The weight of the test specimens was measured during the test. At the start of the test the specimens were 3...6 months old.

$$\text{Durability factor} = \frac{(\text{ultrasound speed during the test})^2}{(\text{ultrasound speed before the test})^2} \quad (6)$$

5.2 Pore Structure of Hardened Concrete

The air content and the average distance between air pores in hardened concrete were calculated using an automatic optical air pore analysis /13/. Results are shown in table 2.

The protective pore ratio was measured using the pressure method /12/ and the capillary water absorption method /14/. Protective pores are those which are not filled with water at normal pressure. Test results are shown in table 2.

Table 2. Test results of hardened concrete.

Concrete	Optical air pore analysis		Protective pore ratio		Number of cycles when durability factor was less than 2/3
	Average distance between air pores (mm)	Air content (%)	Pressure method	Capillary absorption method	
Preliminary mixes:					
Ordinary Portland cement	0.22	3.2	0.24	0.20	37
Portland blast furnace slag cement	0.16	4.2	0.38	0.40	86
Ordinary Portland cement + 8 % silica fume I	0.19	3.4	0.36	0.36	44
- " - II	-	-	0.40	0.45	46
PARTEK I	0.35	0.9	0.20	0.13	30
PARTEK II	0.16	3.3	0.31	0.29	68
PARTEK III	0.24	3.1	0.32	0.25	67
PARTEK IV	0.07	9.5	-	-	105
LIGHTHOUSE	0.15	4.9	-	0.49	56
Test mixes:					
Portland blast furnace slag cement					
slag cement 1	0.18	1.0	0.17	0.18	47
- " - 2	0.22	2.9	0.19	0.16	34
- " - 3	0.17	4.1	0.37	0.44	87
- " - 4	0.09	12.6	0.61	0.66	186
- " - 5	0.11	5.0	0.49	0.58	144
- " - 6	0.09	10.1	0.57	0.52	122
- " - 7	0.12	9.2	0.63	0.73	133
Portland blast furnace slag cement + 8 % silica fume					
slag cement 1	0.34	0.5	0.13	0.16	25
- " - 2	0.14	2.0	0.14	0.14	55
- " - 3	0.14	6.1	0.27	0.26	33
- " - 4	0.10	6.0	0.31	0.38	140
- " - 5	0.07	6.6	0.38	0.44	140
- " - 6	0.07	6.3	0.42	0.46	135
- " - 7	0.10	10.6	0.48	0.46	75
Blended cement					
+ 8 % silica fume 1	0.19	3.2	0.24	0.20	64
- " - 2	0.12	6.4	0.39	0.35	220
Ordinary Portland cement					
1	0.14	2.3	0.22	0.35	80
- " - 2	0.15	4.1	0.28	0.41	78
- " - 3	0.15	3.4	0.30	0.41	89
Ordinary Portland cement + 8 % silica fume					
1	0.18	2.9	0.22	0.30	92
- " - 2	0.14	4.5	0.33	0.36	210
- " - 3	0.09	7.2	0.38	0.43	350

5.3 Other Tests

Air content and consistency of fresh concrete and the compressive strength at the age of 91 days are shown in Table 1.

6. TEST RESULTS

The test method developed was found to be suitable for testing the freezing and thawing resistance of concrete in arctic offshore conditions. It was also found to be very severe. The weakest specimens were destroyed after 25 cycles, the best after 330 cycles. It should be noted that all the specimens tested were made of air-entrained, high strength, superplasticized concrete. In the judging of deterioration by ultrasonic sound velocity, the concrete was considered to be destroyed when the average durability factor was less than 2/3. When judging by weight loss, the criterion was 5 % weight loss. It was found that both criteria gave very much the same results. In Figure 6 examples of the test results are shown. Figure 6 shows the relation between durability and average distance between air pores.

According to the test, the best indicator for the frost resistance of the concrete was the average distance between air pores.

Since the frost resistance of concrete depends on the type of binder used, the average distance between the air pores to achieve the desired frost resistance varies according to the type of binder. The effect of the binder was determined by putting the values obtained from the actual tests into the formula representing the frost resistance and distance between air pores and finding a binder coefficient for each type of binder using the regression analysis. This binder coefficient indicates the ratio of the required distance between the air pores in concrete made from Portland cement to other concrete grades at constant frost resistance.

Corresponding theoretical binder coefficients were also determined on the basis of the hydraulic pressure theory and the theory of capillary ice lens growth as well as the results of the porosity measurements according to the theory of hydraulic pressure. The binder coefficients are listed in table 3. The abbreviations for the various binders are as follows:

PC	= Portland cement
PC+S	= Portland cement + silica 8 %
PBFSC	= Portland blast furnace slag cement
PBFSC+S	= Portland blast furnace slag cement + silica 8 %
BC	= Blended cement (50 % slag)
BC+S	= Blended cement + silica 8 %

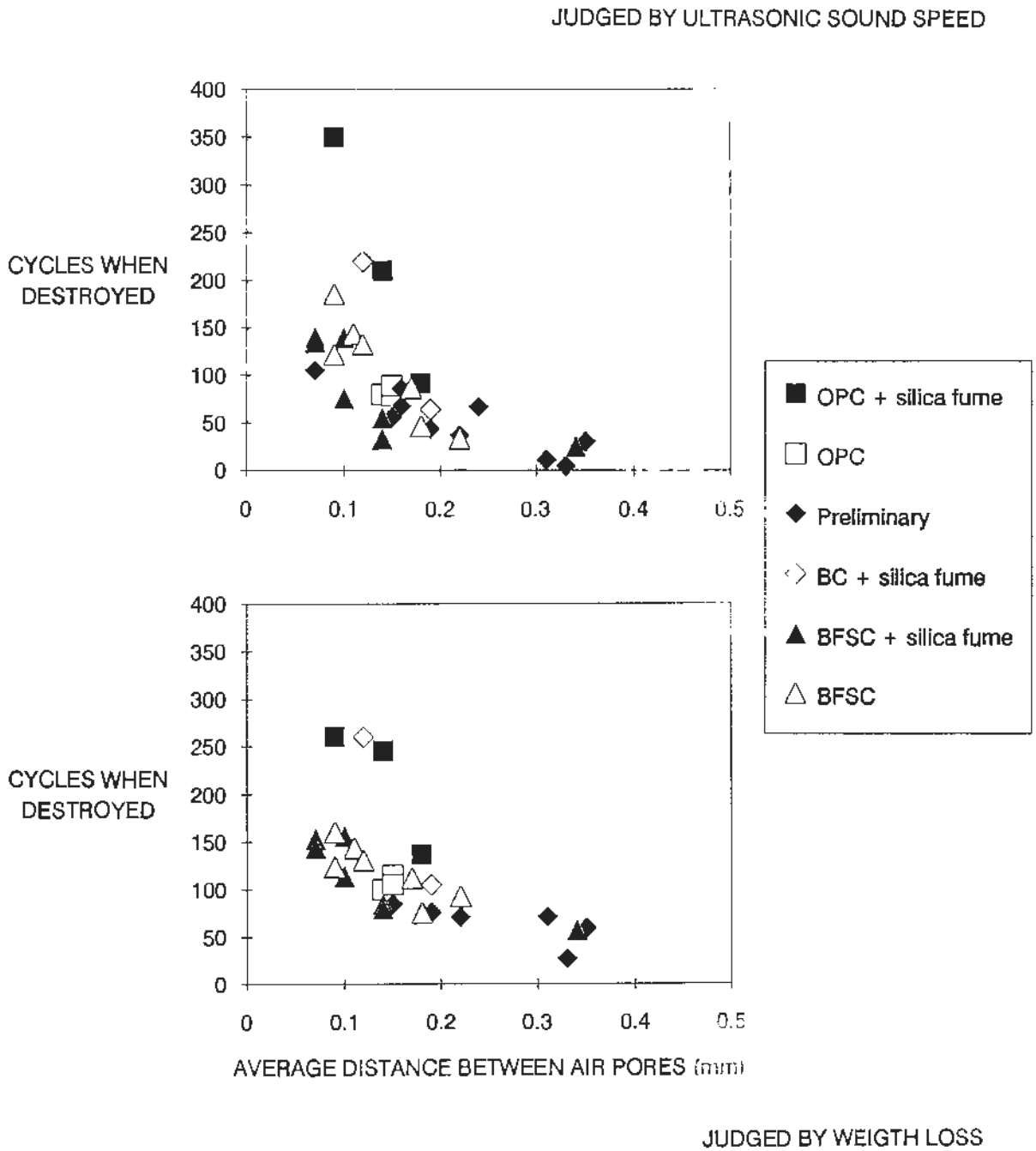


Figure 6. Relation between durability in freezing and thawing test and the average distance between air pores.
OPC = Ordinary Portland cement
BFSC = Blast furnace slag cement
BC = Blended cement.

Table 3. Binder coefficients for spacing factor and average air pore distance for various binders obtained in calculations /5/.

Binder	Tests	Hg porosity measurement	Theoretical	
			Hydr.	Capill.
PC	1	1	1	1
PC+S	1,61	1,30	1,24	1,04
PBFSC	0,99	0,90	1,06	0,91
PBFSC+S	0,70	0,85	-	-
BC	-	-	1,06	0,96
BC+S	1,49	1,15	-	-

The equivalent average distance between air pores irrespective of the type of binder with respect to frost resistance is obtained from equation (7).

$$l_{eq} = \frac{l_m}{\text{binder coefficient}} \quad (7)$$

where l_{eq} = equivalent average distance between air pores
and l_m measured average distance between air pores.

Fig. 7 shows the interdependence obtained for frost resistance and the equivalent average distance between the air pores.

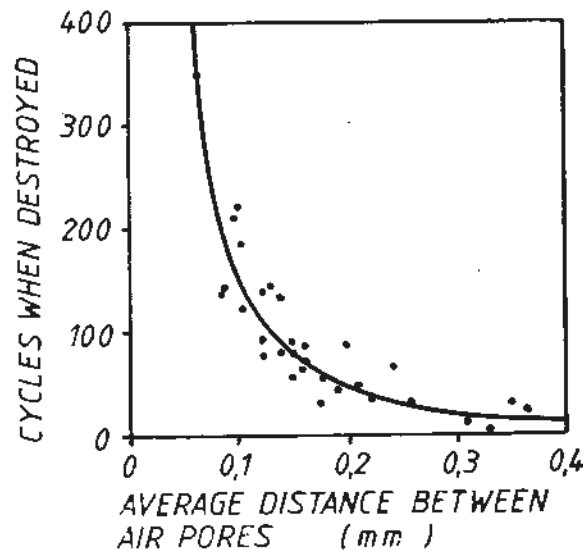


Fig. 7. Interdependence between arctic freezing-thawing resistance and the average distance between air pores in a concrete standardized to correspond to Portland cement on the basis of the speed of ultrasonic sound /27.

As the figure indicates, the scatter of the test results processed in this way is relatively low. The highest scatter is due to results obtained in the preliminary tests. We may conclude that, at a constant water-cement ratio, the average distance between the air pores correlates, with reasonable accuracy, the frost resistance of concrete in arctic freezing and thawing tests.

The various binders behaved in tests as they could theoretically be expected to behave. However, the effect of silica was far greater than calculated.

When comparing the computed theoretical requirements to experimental values, we obtain the comparison processed in Fig. 8.

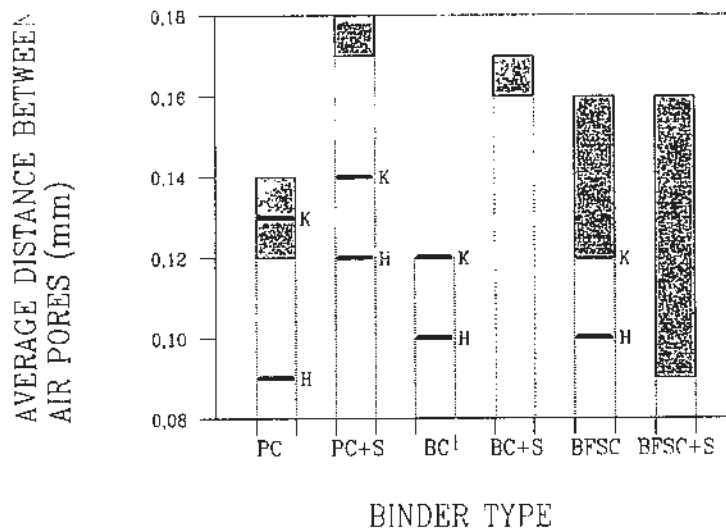


Fig. 8. Comparison of theoretically and experimentally determined average distances between air pores. The shaded area indicates the range of experimental values. Values marked with H refer to figures computed according to the hydraulic pressure theory and those marked with K to figures computed according to the theory of capillarity ice lens growth /5/.

When comparing the values shown in Fig. 8, we can see that the limits for the average air pore distances for Portland cement (PC), Portland cement + silica (PC+S) and Portland blast furnace slag cement (PBFS) correspond with relatively high accuracy to the values determined in accordance with the theory of the capillarity ice lens growth. According to the hydraulic pressure theory, these values are too low.

So the test results support the theory of capillarity ice lens growth. Therefore this theory could well be used as a basis for the comparison of various binders, concrete mixes and environmental conditions.

In the tests, silica improved the frost resistance of concrete considerably. In fact, this improvement was greater than theoretically expected. However, it should be noted that Portland cement and blended cement mixed with silica was studied only in a couple of mixes. Therefore it is advisable not to expect silica to improve frost resistance to the extent indicated by the tests. Further tests and field experience are required to show whether silica really improves frost resistance as much as this.

The requirements presented should be applied only to concrete mixes with a water-cement ratio of about 0.35 as used in the tests. If the water-cement ratio is other than this, new limits should be established either by means of experiments or along the lines presented in the theory section of this paper.

As a example of the effect of the water-cement ratio, we present in Fig. 9 the interdependence between arctic freezing and thawing resistance of concrete and the average spacing of air pores at various water-cement ratios. The interdependence reflecting the water-cement ratio of 0.35 was obtained from Fig. 7. This dependence has been converted to match other water-cement ratios in accordance with the principles of the capillarc ice lens growth theory.

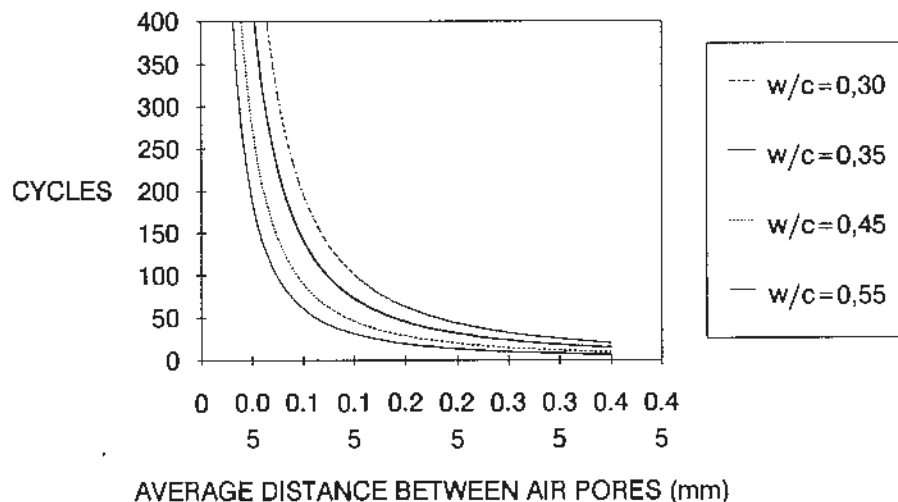


Fig. 9. Effect of the water-cement ratio on the arctic freezing and thawing resistance of concrete computed according to the theory of the growth of capillarc ice crystals.

7. REFERENCES

1. Bager, D. H. Ice formation in hardened cement paste. Lyngby 1984, Technical University of Denmark, Building Materials Laboratory, Technical Report 141/84. 66 s.

2. Castellan, G. W. Physical chemistry. 3rd ed. Reading, MA 1983, Addison-Wesley. 1000 s.
3. Collins, A. R. The destruction of concrete by frost. Journal of the Institution of Civil Engineers 1944:23, s. 29 - 41.
4. CRC handbook of chemistry and physics. 63rd ed. Boca Raton, Fla. 1982, CRC Press. 2000 s.
5. Leivo, M. Frost resistance of concrete in arctic offshore structures. Espoo 1989, Technical Research Centre of Finland, Research Report 621. 136 p. (In Finnish)
6. Leivo, M. Frost-resistance of concrete in very low temperatures. Espoo 1988, Technical Research Centre of Finland, Research Report 536. 31 p. + app. 8 p. (In Finnish)
7. Litvan, G. G. Pore structure and frost susceptibility of building materials. Ottawa 1973, National Research Council Canada, Division of Building Research, Research Paper 584. S. 17 - 30.
8. Powers, T. C. Freezing effects in concrete. In: Durability of concrete. Detroit, Mich. 1975, American Concrete Institute, Publication SP-47. S. 1 - 11.
9. Powers, T. C. Resistance of concrete to frost at early ages. Chicago 1956, Portland Cement Association, Research and Development Laboratories, Research Department, Bulletin 71. 47 s.
10. Powers, T. C. & Helmuth, R. A. Theory of volume changes in hardened portland-cement paste during freezing. Proceedings, Highway Research Board 32(1953)5, s. 285 - 297.
11. Powers, T. C. The air requirement of frost-resistant concrete. Chicago 1949, Portland Cement Association, Research and Development Laboratories, Development Department, Bulletin 33. 28 s.
12. SFS 4475. Concrete. Frost resistance. Protective pore ratio. Finnish Standards Association, 1988. 2 s. (In Finnish)
13. Vesikari, E. Image analysis in determining pore size distributions of concrete. Espoo 1985, Technical Research Centre of Finland, Research Notes 437. 31 p.
14. Vesikari, E. Critical degree of saturation - a new concept for estimating concrete frost resistance. Betonituote 1981:3, s. 49 - 51. (In Finnish)